Pollution sources identification, health, and radiological risk assessment of naturally occurring radioisotopes and heavy metals in waste dumpsites in Ijebu-Ode, Ogun State, Southwest Nigeria

Gbadamosi, M. R.; Abayomi, A. A.; Afolabi, T. A.; Adegboye, M. A.; Bakare, H. O.; Banjoko, O. O.; Ogunneye, A. L.; Ugbomeh, I. L.; Jegede, D. O.; Ajetunmobi, A. E.; Bakare, T. E.

DOI:
10.1080/15275922.2021.2006365

Pollution sources identification, health, and radiological risk assessment of naturally occurring radioisotopes and heavy metals in waste dumpsites in Ijebu-Ode, Ogun State, Southwest Nigeria

Gbadamosi, M. R[a, g,*]., Abayomi, A. A[b]., Afolabi, T. A[c]., Adegboye, M. A[d]., Bakare, H.O[e]., Banjoko, O. O[a]., Ogunneye, A. L[a]., Ugbomeh, I.L[f]., Jegede, D.O [g]., Ajetunmobi, A.E [h]., and Bakare, T.E [i].

[a,g] Department of Chemical Sciences, Tai Solarin University of Education, Ijagun, Ijebu-Ode, Nigeria

[b] Department of Chemistry, University of Lagos, Lagos, Nigeria

[c] Department of Chemistry, Federal University of Agriculture Abeokuta, Ogun State, Nigeria

[d] Department of Computer Engineering, Federal University, Oye-Ekiti, Nigeria

[e] Post-Doctoral Research Fellow (ASAP East Africa Project, University of Birmingham, UK)

[f] School of Geography Earth and Environmental Science, University of Birmingham, UK

[g] Department of Basic Science, Chemistry Unit, Babcock University, Ogun State, Nigeria

[h] Department of Physics, Olabisi Onabanjo University, Ago-Iwoye, Ogun State, Nigeria

[i] Department of Chemistry and Biochemistry, Caleb University, Imota, Lagos State, Nigeria

Abstract

This study evaluates human health, pollution, and radiological risk assessment of potentially toxic metals (PTMs) (Pb, Cd, Cr, Ni and Zn), radioisotopes (^{238}U, ^{232}Th and ^{40}K) and its associated radiological indices from dumpsite soils in Ogun State, Nigeria, using a calibrated atomic absorption spectrophotometer (AAS) and highly shielded γ-ray spectrometry using NaI(TI) detector. Fourier transform infrared spectrometer (FTIR) complemented by X-ray diffraction (XRD) techniques were

used to evaluate the mineralogical composition of the soils. Multivariate statistical analysis was used to apportion the source of PTMs and the radioisotopes. The mean concentration of Pb, Cd, Cr, Ni and Zn obtained were 22.35, 17.95, 20.83, 19.02 and 75.88 mg kg^{-1}respectively. The activity concentrations of ^{238}U, ^{232}Th and ^{40}K ranged from 49.71 ± 16.3 - 314.15 ± 55.2, BDL - 87.54 ± 7.38 and BDL - 3721.3 ± 231.6 $Bqkg^{-1}$respectively. The values obtained were above the global average value in most of the samples. According to the four-pollution and ecological risk assessment model, the dumpsite soils is strongly to low polluted and enriched with toxic metals in the order Zn > Cr > Pb > Ni > Cd. The estimated carcinogenic risk of the three carcinogenic PTMs for children and adults were higher than the acceptable limit (1×10^{-6}). The results of the PCA and HCA results are consistent with the correlation coefficient analysis which showed that mixed natural, anthropogenic and lithogenic sources mainly from aggregation of lead-containing materials in the waste on the dumpsite, vehicular emission and industrial discharges are the main sources of Pb, Ni and Cd in the three studied dumpsites. Thus, dumpsite soil poses great threat to health, increased pollution and enhances the radiological risk to the general population via human multiple exposure routes.

Keywords: Toxic metals; Radiological risk; Geo-accumulation; Mineralogical and Carcinogenic risk

1. Introduction

The steady increase in the volume of waste generated, coupled with the inefficient waste disposal and recycling processes in Nigeria, have continued to exacerbate the risk of potential toxic metals (PTMs) and radioisotopes contamination of the soil and water bodies. This has led to increased exposure of abiotic and biotic components of the nation's ecological systems to possible degradation, and several debilitating challenges posed to the well-being of city residents (Njoroge, 2007). Major cities in Nigeria struggle to manage physical waste efficiently while chemical and other hazardous wastes and

their impacts do not get deserved attention (Adeyemi, 2011; Ikporupko, 2018). Possible hazards from waste dumpsites are not only in terms of the obnoxious poisonous gases, odour and presence of pathogens being released, but can also include radiation emanating from the sites (Gbadamosi *et al.,* 2017; Ojoawo *et al.,* 2011). Soil is the main receiver of solid wastes and thus acts as a sink for radioisotopes, potential toxic metals (PTMs) and other emerging organic and inorganic pollutants of environmental and health concerns which are eventually embedded into the soil (Nyles and Ray, 1999). Several studies have shown that most of the synthetic and electronic waste (e-waste) that are found in open dumpsites contain toxic elements that are harmful to humans, plants and animals (Jibiri *et al.,* 2014). Plant absorption of these pollutants and their incorporation into the food chain is one of many indices used for calculating exposures frequency and performing human health risk assessment (Zach, 1982; Wadey *et al.,* 1991). Radioisotopes, potentially toxic metals (PTMs) and other emerging organic and inorganic contaminants in foods from impacted soil can damage human health through various absorption and biochemical pathways (Mamut et al., 2017). Long-term exposures to carcinogenic metals and radioisotopes through multiple exposure routes could lead to serious health effects such as chronic lung diseases, acute leucopoenia, anaemia and necrosis of the mouth (Ramasamy *et al.,* 2013). ^{232}Th exposure can cause lung pancrease, hepatic, bone and kidney cancers and leukaemia (Taskin *et al.,* 2009).

Ijebu-Ode metropolis, being a densely populated city in Nigeria, generates a large amount of electronic and non-electronic solid waste materials which are disposed-off in open sites without any soil protection measures (Solaja et al., 2017). The solid wastes end up interacting with the soil particles, thereby changing the soil physicochemical properties (Piccolo and Mbagwu, 1997). The increased volume of wastes generated in most Nigerian urban settlements necessitates the need to correctly assess the risk posed by these wastes, suggest effective waste disposal legislation and

institute possible mitigating measures to arrest likely impacts on human health, plants, and animals. Therefore, the objectives of the present study include (i) determination of the activity concentrations and spatial distribution of waste enhanced naturally occurring radioisotopes materials (WENORM) ^{238}U, ^{232}Th and ^{40}K in the representative soil samples from the selected dumpsite in Ijebu-Ode, Southwest Nigeria (ii) to evaluate the pollution and ecological risk levels based on the waste (iii) to evaluate the carcinogenic and non-carcinogenic risk of identified PTMs, radioisotopes and associated radiological parameters via multiple exposure pathways in the soil samples from the dumping sites (iv) identify and apportion the main source of radioisotopes and heavy metals pollution and (v) establish the relationship between the PTMs radioisotopes and their associated radiological and health risk parameters. Thus, this study will facilitate the establishment of a reliable baseline data for the heavy metals, radioisotopes, and its associated parameters in a typical dumpsite in Southwestern Nigeria.

2. Materials and Methods

2.1 Description of the study area

Ijebu-ode is a densely populated town located within latitude 6°45′0′ N and 6°50′′ North of the equator and longitude 3°50′′ E and 4°00′′ East of the Greenwich Meridian (Figure 1). It is situated at 110 km north-east of Lagos and within 100 km radius of the Atlantic Ocean from the Eastern fringes of Ogun State (Nigeria) and Dahomey basin (Benin Republic). The Dahomey basin envelopes a substantial part of the continental margin of Gulf of Guinea, stretching from Volta-delta in Ghana (West) to the Okiti-pupa ridge in Nigeria (East) (Nton et al., 2009). Dahomey basin is much of a geological interest due to the reported discovery of valuable mineral deposits within the region (Nton, 2009). Three major wastelands/dumpsites within the city were used for the study. These study locations were Ikoto

dumpsite (IAS) along Benin-Sagamu Expressway, Ikangba Estate dumpsite (IBS) and Olisa dumpsite (ICS) respectively.

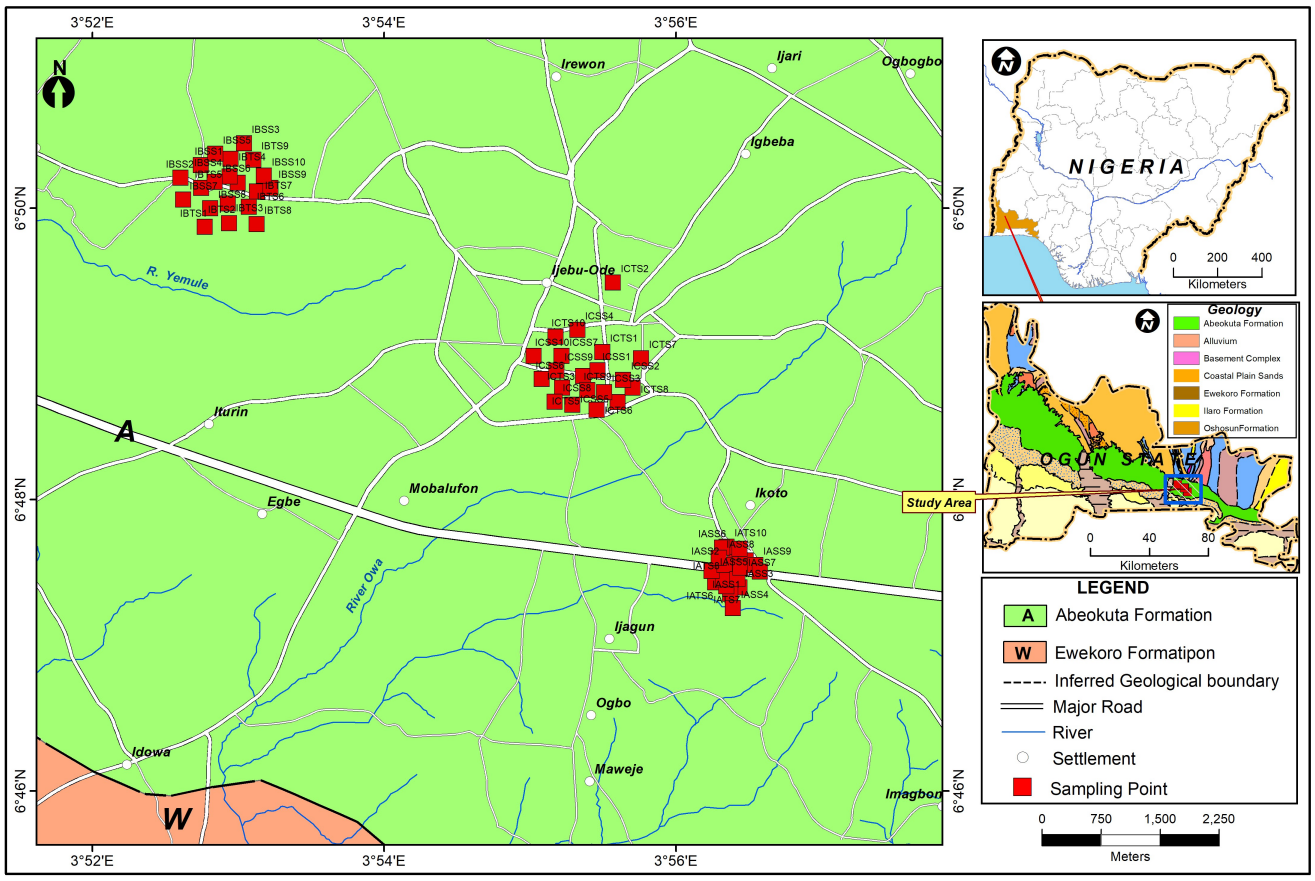

Fig. 1: Map of the Study area showing the Sampling locations

2.2 Soil sample collection and preparation

The study areas Ikoto, Ikangba and Olisa dumpsites are located within the latitude 03°52′890″N and 03°56′360″ North of the Equator and longitude 06°47′169″E and 06°48′876″ East of the Greenwich Meridian. A total of sixty (60) soil samples were obtained from the three dumpsites between May-June 2018 and July 2019 at 0 – 10 cm depth, using a hand driven soil auger. Two waste free control samples within the same geological formation with the dumpsites were also sampled. In each location, the dumpsite was divided into two sections and twenty sub-samples were collected and composited

from each section to obtain representative 10 samples for the top and sub-soil respectively using coning and quartering technique. Thus, twenty representative soil samples were obtained from each dumpsite and three control soil samples without any anthropogenic input were also collected. The soil samples were placed in a new labeled polythene bags and immediately taken to the laboratory. Their respective sample locations were recorded using a hand-held Global Positioning System (GPS) (Model GARMIN GPS-13). Samples were air-dried separately within a controlled chamber at room temperature for a month to avoid further atmospheric deposition and cross contamination, and then pulverized before made to pass through 60 mesh sieves after removing the stones and debris.

2.2.1 Potential toxic metals (PTMs) Digestion Procedure and Radioisotope measurements

For the PTMs determination, 1 g of soil samples were digested and spiked with a standard solution of the five metals for about 1 hour in a ternary mixture of 3:2:1 nitric acid (HNO_3), perchloric acid ($HClO_4$) and Hydroflouric acid (HF) respectively, as described by (Gbadamosi *et al.,* 2018a; Liu *et al.,* 2013). The concentrations of the PTMs were then determined using Buck Scientific (Model 210 VGP) Atomic Absorption Spectrophotometer (AAS). The results obtained were compared with those of the un-spiked dumpsite soil samples. The percentage recovery of the spiked soil samples were 89.3 % for Pb, 92.4 % for Cd, 97.4 % for Cr, 91.2 % for Ni and 86.5 % for Zn, respectively. The limits of detection (LOD) were 0.08, 0.01, 0.04, 0.05 and 0.15 for Pb, Ni, Cd, Cr, and Zn and the limits of quantification (LOQ) were 0.26, 0.03, 0.13, 0.17 and 0.50 mg/kg for Pb, Ni, Cd, Cr, and Zn respectively. For the PTMs determination, the absorbance value for blank and working standard solution were also measured.

For radioisotopes measurement of the dumpsite soil samples, two hundred grams (200 g) of each prepared soil samples were packed into cleaned and labeled cylindrical glass vessels and then placed in transparent polyethylene bags and sealed. These samples were safely conveyed to National

Institute of Radiation Protection and Research (NIRPR), University of Ibadan, Ibadan, Southwest Nigeria. At the laboratory, the plastics were hermitically sealed with sticky tape and kept for 40 days to ensure that the parent and daughter nuclides in the sample were at secular equilibrium between radium and its gaseous decay progenies. At the end of this equilibrated period, the samples were subjected to gamma-ray spectrometer.

2.2.2 Quality control and statistical analysis

For quality assurance and quality control (QA/QC), reagent blanks and sample duplicates were incorporated in the analysis to detect any contamination in the analytical materials and to assess precision and bias in the method of analysis. The recoveries ranged from 86.5 % to 97.4 %. Samples were carefully conveyed to the laboratory in a sealed compartment. All glassware, sample collection materials and digestion vessels were pre-washed with soap less detergent, soaked with dil. HNO_3 (1+1) and then thoroughly rinsed in tandem with double distilled and deionized water. All the reagents used were of high purity analytical grade. Univariate and multivariate statistical analyses were used for the analysis of radioisotopes and PTMs in the soil samples. The univariate analysis includes, mean, maximum, minimum, standard deviation, coefficient of variation, standard error of the mean (SEM), skewness and kurtosis. The multivariate statistical analyses (MVA) such as principal component analysis (PCA), hierarchical cluster analysis (HCA) and correlational analysis were employed to apportion and differentiate the sources of the PTMs and radioisotopes and establish the mutual influence of the variables on each other. This according to Tahri et al. (2005), will allow the determination of the relationship between radioisotopes and their associated radiological and health parameters and PTMs in order to establish their common origin using the commercial statistics software package IBM SPSS statistics (version 26, Inc., Chicago IL). MATLAB software was used for the spatial distribution of the radioisotopes and PTMs in the samples.

2.3 Radioisotopes Analysis

2.3.1 Sample measurements

Radioisotopes ^{238}U, ^{232}Th and ^{40}K activity concentrations were quantified by a well calibrated γ-ray spectrometry using NaI (TI) detector. The counting assembly for the natural radioisotopes determination made up of a scintillation detector coupled to a Canberra multi-channel analyzer which consists of 7.6 mm x 7.6 mm NaI (TI) detector (Model Bicron) with adequate lead shielding which reduced the background by a factor of about 0.95. The γ-ray spectrometer was calibrated appropriately (energy and efficiency calibration) and tested for its linearity using the well-calibrated standard gamma source outsource from the International Atomic Energy Agency (IAEA), laboratories, Vienna, Austria (Ademola et al., 2008). The resolution of the NaI (TI) detector is 7.5 % at 0.662 MeV of ^{137}Cs. Each of the samples was measured for 18 000 sec in order to obtain good statistics for the radioisotopes. Also, measurements were repeated at intervals for quality control and assurance purposes as well as to maintain the stability of the counting system. The background radiation due to the radioisotopes in the vicinity around the detector was measured using an empty plastic container, which was measured in the same manner as the soil and reference sample (Jibiri et al., 2014). The net radioisotopes activity concentrations were obtained by subtracting the background spectrum from the measured spectra. Three intensity regions were identified in the spectrum which corresponds to 1.460 MeV for (^{40}K) content, 1.760 MeV for (^{214}Bi) and ^{232}Th content determined from 2.614 MeV for (^{208}TI) in the samples. The below detectable limit (BDL) of each radionuclide were determined from the background radiation spectrum for the same counting time as was done for the dumpsite soil samples and are given as 0.037 Bq kg^{-1} for ^{238}U, 0.007 Bq kg^{-1} ^{232}Th and 0.18 Bq $kg^{-1}$for ^{40}K respectively.

2.4 Radiological and health hazard parameters

In order to evaluate the γ-ray radiation and health hazards impact of the radioisotopes ^{238}U, ^{232}Th and ^{40}K in the dumpsites and consider the radiological hazards of the soil to humans, suitability of the soils for building constructions, farming, remediation and other purposes. Even though total activity concentrations of radioisotopes were determined, it does not provide the exact indication of the total radiation hazard. Therefore, a comprehensive estimation of these radiological and health hazard parameters to humans become necessary. Table S1 gives details formulas for each radiological and health hazard index evaluated in this present study.

2.5 Assessment of Potentially toxic metals Pollution and Ecological Risk

Several approaches have been used to evaluate the pollution, contamination and ecological risk of PTMs in the soil. In this present study, four of these indices such as index of geo-accumulation (I_{geo}), contamination factor (CF), pollution loading index (PLI) and potential ecological risk index (PERI) were extensively used to evaluate the pollution and ecological risk of the soil to biological organisms in the environment.

2.5.1 The index of geo-accumulation (Igeo)

The Index of geo-accumulation (I_{geo}) was used to evaluate potentially toxic metals (PTMs) pollution levels resulting from anthropogenic activity based on the use of a single toxic metal in the soils (Men et al., 2018). The index has been widely applied in European trace metals since the late 1960 and is defined as follows:

$$I_{geo} = \log_2\left(\frac{C_n}{1.5\,B_n}\right) \quad (1)$$

Where C_n and B_n are the levels of potentially toxic metals, n, in the soils and the geochemical background levels of the corresponding toxic metals n respectively. The constant 1.5 represents the correction factor due to anthropogenic/lithogenic effects (Tian et al., 2017).

192 The following classifications were used for Igeo: Igeo value > 5 (extremely polluted), Igeo between 4
193 and 5 (heavily-extremely polluted), Igeo between 3 and 4 (strongly polluted), Igeo between 2 and 3
194 (moderately-strongly polluted), Igeo values between 1 and 2 (moderately polluted), Igeo between 0
195 and 1(unpolluted-moderately pollution), Igeo value ≤0 (unpolluted) (Hua et al., 2018).
196
197 **2.5.2 Contamination Factor and Pollution Loading Index**
198 Contamination factor (CF) is a vital contamination evaluation method that determined the degree of
199 contamination of the sampling site by PTMs (El-Amier *et al.,* 2017). The CF of each metal is
200 calculated as the ratio of individual toxic metal concentrations to the background values, and is
201 defined by this equation (Bourliva et al., 2018; Gbadamosi et al., 2018a).
202 $$\text{Contamination Factor} = \frac{(C_{metal})_{sample}}{(C_{metal})_{background}} \quad (2)$$
203 CF is ranking from 1-6 was used to evaluate the level of contamination based on the strength: CF ≤ 0:
204 non-contaminated, 0 < CF ≤ 1: slightly contaminated; 1 < CF ≤ 3: moderately contaminated; 3 < CF ≤
205 5: considerately contaminated; 5 < CF ≤ 6: strongly contaminated; CF > 6: very strongly
206 contaminated. (Gabarrón *et al.,* 2017).
207 **2.5.3 Pollution loading index (PLI)**
208 PLI allow an easy but relative means of evaluating the total pollution and quality of the soil from the
209 selected sites (Chakravarty and Patgiri, 2009). It is mathematically defined as the nth root of the
210 multiplication of contamination factors (CFn) expressed as follows:
211 $$PLI = (CF_1 x\, CF_2 x\, CF_3 x \dots\dots CF_n)^{\frac{1}{n}} \quad (3)$$
212 Where n is the number of PTMs (in the present study, n=5). PLI is a basic and convenient pollution
213 assessment method for toxic metals. The degree of pollution using PLI is classified as follows: PLI <

214 1 (no pollution), low pollution (1 < PLI ≤ 2), moderate pollution (2 < PLI ≤ 3), and heavy pollution
215 (PLI > 3) (Jamal *et al.,* 2018; Gbadamosi et al., 2018a).
216
217 **2.5.4 Potential ecological risk index (PERI)**
218 PERI is a powerful technique for quantitatively express the potential ecological risk posed by
219 individual toxic metals in the selected dumpsites soils. This method considers four pollutants
220 characteristics such as concentration, nature, toxicity, and sensitivity of the pollutants to the water
221 body from the soil (Gbadamosi *et al.,* 2018a; Zhang *et al.,* 2016). PERI can be determined using the
222 formulas:
223 $$\text{PERI} = \sum_{i=1}^{n} E_r^i = \sum_{i=1}^{n} T_r^i \times C_f^i = \sum_{i=1}^{n} T_r^i \times \frac{C_m^i}{C_b^i} \quad (4)$$
224 Where E_r^i is the potential ecological risk factor for each toxic metal, i, T_r^i is the toxic response factor
225 of the individual toxic metals in the dumpsite's soils. C_f^i is the contamination factor of the toxic
226 metals, C_m^i and C_b^i are the concentrations of the toxic metals in the sample and background value of the
227 metals, respectively. Based on literature, T_r^i for Pb, Cd, Cr, Ni and Zn are 5, 30, 2, 5 and 1,
228 respectively (Zhang *et al.,* 2016). PERI is categorized into four as: PERI < 150 (low ecological risk),
229 150≤PERI < 300 (moderate ecological risk), 300≤PERI < 600 (high ecological risk) and PERI > 600
230 (very high ecological risk) (Tian *et al.,* 2017).
231
232 **2.6 Human Health risk assessment**
233 The human health risk models including the carcinogenic and non-carcinogenic risk estimation of the
234 various organic and inorganic pollutants were developed by USEPA and have been globally adopted
235 (USEPA, 2011; 2002). Three human exposure pathways were used to estimate the human average
236 daily dose (ADD) of the potentially toxic metals (PTMs) via ingestion, inhalation and dermal

absorption using the equation provided in Table S2. A detailed explanation of the mathematical formulas was presented in Table S2.

The Hazard quotient (HQ) is widely used to determine the non-carcinogenic risk assessment for a single metal or hazard index (HI) for multiple metals via multiple exposure pathways. This is calculated as the ratio of the average daily dose (ADD) and the reference dose (RfD) for a given metals.

$$\text{HQ (dimensionless)} = \frac{\text{Average daily dose during exposure to PTMs (ADD)(mg kg}^{-1}\text{day}^{-1})}{\text{RfD (mg kg}^{-1}\text{day}^{-1})} \quad (5)$$

$$\text{HI} = \sum \text{HQ}_i = \sum \frac{\text{ADD}_i}{\text{RfD}_i} \quad (6)$$

HI or HQ determines the magnitude of adverse health effects. Adverse health effects are unlikely to occur if HQ or HI < 1 and the magnitude of risk increases as HI or HQ increases to a unity safe level. High chronic risk effect is indicated if HQ > 10 (USEPA, 2001; 2011; Ogunbanjo et al., 2016).

The carcinogenic risk assessments are determined by estimating the probability of individuals developing any cancer type over time because of prolonged exposure to the carcinogenic agent in the study site. The carcinogenic risk can be estimated using the equation:

$$\text{Cancer risk} = ADD \times PF \quad (7)$$

Where PF ($mgkg^{-1}day^{-1}$) is the potency factor which is the slope of the dose-response curve (Table 3). The cumulative cancer risk can then be calculated from:

$$\text{Total cancer risk (TCR)} = \sum_{i=1}^{n} \text{ADD}_i \text{PF}_i \quad (8)$$

Where PF_i is the potency factor for the metal i ($mg\ kg^{-1}day^{-1}$) and ADD_i is the average daily dose ($mg\ kg^{-1}\ day^{-1}$). The accepted tolerable risk for regulatory purposes is between $1 \times 10^{-6} \leftrightarrow 1 \times 10^{-4}$ (US EPA, 2011; Li *et al.,* 2018). This means that if the estimated cancer risk is lower than 1×10^{-6}, there is

a probability of one chance in a million of an individual's developing cancer over the lifetime and this risk are considered negligible (Li *et al.,* 2018).

2.7 Mineralogical characterization using FTIR and XRD

The mineralogical characterization of the soil was determined using Perkin Elmer RX1 Fourier transform infrared spectrometer (FTIR). The IR spectra for all the samples were recorded in the region 4000-650 cm^{-1}. Sample preparation and procedure for mineral analysis by FTIR were clearly presented in the earlier published work (Gbadamosi et al., 2018b). However, for XRD, the diffraction pattern was determined by Rigaku Ultimate IV X-ray diffractometer with a curve of graphite monochromator and a radiation source of CuKα. The diffraction patterns were obtained in the range of 2θ and region between 20°-80° and with a scan speed of 1°/min. The obtained XRD patterns for the samples were processed by matching the diffraction patterns with a joint committee on powder diffraction standard (JCPDS) database (Berry, 1974).

3 Results and Discussion

3.1 Activity concentrations of radioisotopes and radiological characterization of the dumpsites soil samples

Table 1: Statistical summary of the Activity concentration and Radiological Characterization of dumpsite soil samples (n=60) and control (n=2).

	Arithmetic mean	Maximum	Minimum	Standard deviation	CV (%)	SEM	Skewness	Kurtosis	World average[a]
Concentration of ^{238}U(Bqkg^{-1})	142.20 ± 25.9	314.15 ± 55.2	49.71±16.3	60.7	36.1	7.83	1.09	0.91	33
Concentration of ^{232}Th(Bqkg^{-1})	16.11 ± 3.00	87.54 ± 7.38	BDL	17.3	90.4	2.23	2.53	8.32	45
Concentration of ^{40}K(Bqkg^{-1})	362.30± 27.6	3721.3 ± 231.6	BDL	580	148.8	74.9	4.24	24.2	420
Absorbed dose rate D_R (nGyhr^{-1})	90.54 ± 14.9	215.95 ± 25.6	40.64 ± 10.6	35.7	33.8	4.60	1.21	2.42	57
Radium equivalent Raeq(Bqkg^{-1})	193.14±32.3	420.30±55.4	84.9±23.0	74.2	32.9	9.57	0.94	0.97	370
$AEDE_{outdoor}$ (μSvyr^{-1})	111.1±18.3	265.02±31.4	49.88±13	43.8	33.8	5.65	1.21	2.42	70
$AEDE_{indoor}$ (μSvyr^{-1})	444.5±73.3	1060±126	199.5±51.9	175	33.8	22.6	1.21	2.42	450
AGDE (μSvyr^{-1})	620.5±101.2	1577.5±155.6	283.7±71.4	350	34.7	32.3	1.44	3.75	1000
ER (μRhr^{-1})	380.5±62.6	922.1±105.3	172±43.6	151	34.0	19.4	1.24	2.66	600
H_{ext}	0.52±0.10	1.14±0.15	0.23±0.06	0.20	32.9	0.03	0.94	0.96	≤ 1
H_{int}	0.91±0.16	1.70±0.30	0.36±0.11	0.34	32.2	0.04	0.76	-0.11	≤ 1
Iγr	0.68±0.11	1.69±0.19	0.36±0.11	0.34	34.4	0.04	1.36	3.35	≤ 0.5
AUI	1.54±0.28	3.00±0.51	0.58±0.17	0.61	33.8	0.08	0.81	-0.07	≤ 2
ELCRx10^{-3}outdoor	388.9±64.1	928±110	175±45.4	153	33.8	19.8	1.21	2.42	290
Control 1: ^{238}U (Bqkg^{-1})	24.30±11.32								
Control 1: ^{232}Th (Bqkg^{-1})	4.55±0.42								
Control 1: ^{40}K (Bqkg^{-1})	54.20±9.55								
Control 1: D_R (nGyhr^{-1})	16.24±5.88								
Control 1: Raeq (Bqkg^{-1})	34.98±12.66								
Control 2: ^{238}U (Bqkg^{-1})	10.32±5.43								
Control 2: ^{232}Th (Bqkg^{-1})	2.14±0.21								
Control 2: ^{40}K (Bqkg^{-1})	21.32±5.61								
Control 2: D_R (nGyhr^{-1})	6.95±2.87								
Control 2: Raeq (Bqkg^{-1})	15.02±6.16								

[a] UNSCEAR (2000); BDL = Below Detection Limit

The value of the activity concentrations due to the naturally occurring radioisotopes ^{238}U, ^{232}Th and ^{40}K ranged from 49.71 ± 16.3 Bq kg^{-1} - 314.15 ± 55.23 Bqkg^{-1}, BDL - 87.54 ± 6.75 Bqkg^{-1} and BDL - 3721.25 ± 231.57 Bq kg^{-1} with an average value of 142.20 ± 25.9, 16.11 ± 3.00 and 362.30 ± 27.6 Bq kg^{-1}respectively (Table 1). It was observed that in all the soil samples activity concentrations of radioisotopes ^{238}U were about 2 to 11 times higher than the world average value of 33Bq kg^{-1} (UNSCEAR, 2000) (Fig. 2). The average activity concentrations of ^{238}U were about 5 times higher than the world average value in the dumpsites. Activity concentrations of ^{232}Th in soil samples were below the world average value of 45 Bq kg^{-1} except for soil sample ICTS5, ICTS10, ICTS2 and ICTS3 with activity concentrations of 45.21 ± 3.50 Bq Kg^{-1}, 53.21 ± 5.52 Bq Kg^{-1}, 76.89 ± 7.38 Bq Kg^{-1}, and 87.54 ± 6.75Bq Kg^{-1}, which are 1-2 times higher than the world average value. The activity concentrations of ^{40}K in all the top and sub soil samples from Ikoto dumpsite exceed the world average value of 420 Bq kg^{-1}. More so, five and one soil samples from Ikangba and Olisa dumpsites respectively have higher ^{40}K values than the recommended limit of 420 Bq Kg^{-1} (Fig. 2). The average values of the ^{40}K radioisotope were higher than the world average value of 420 Bq kg^{-1} in all the samples. In all sampling locations, the activity concentrations of the radioisotope were in the order: $^{40}K > ^{238}U > ^{232}Th$ (Fig. 2). In few of the sampling points, the activity concentrations of ^{40}K and ^{238}U were extremely high; this may be attributed to the extensive use of NPK fertilizer, the solubility and mobility of uranium rich rock or the large deposit and aggregation of clinical wastes containing uranium in the study areas.

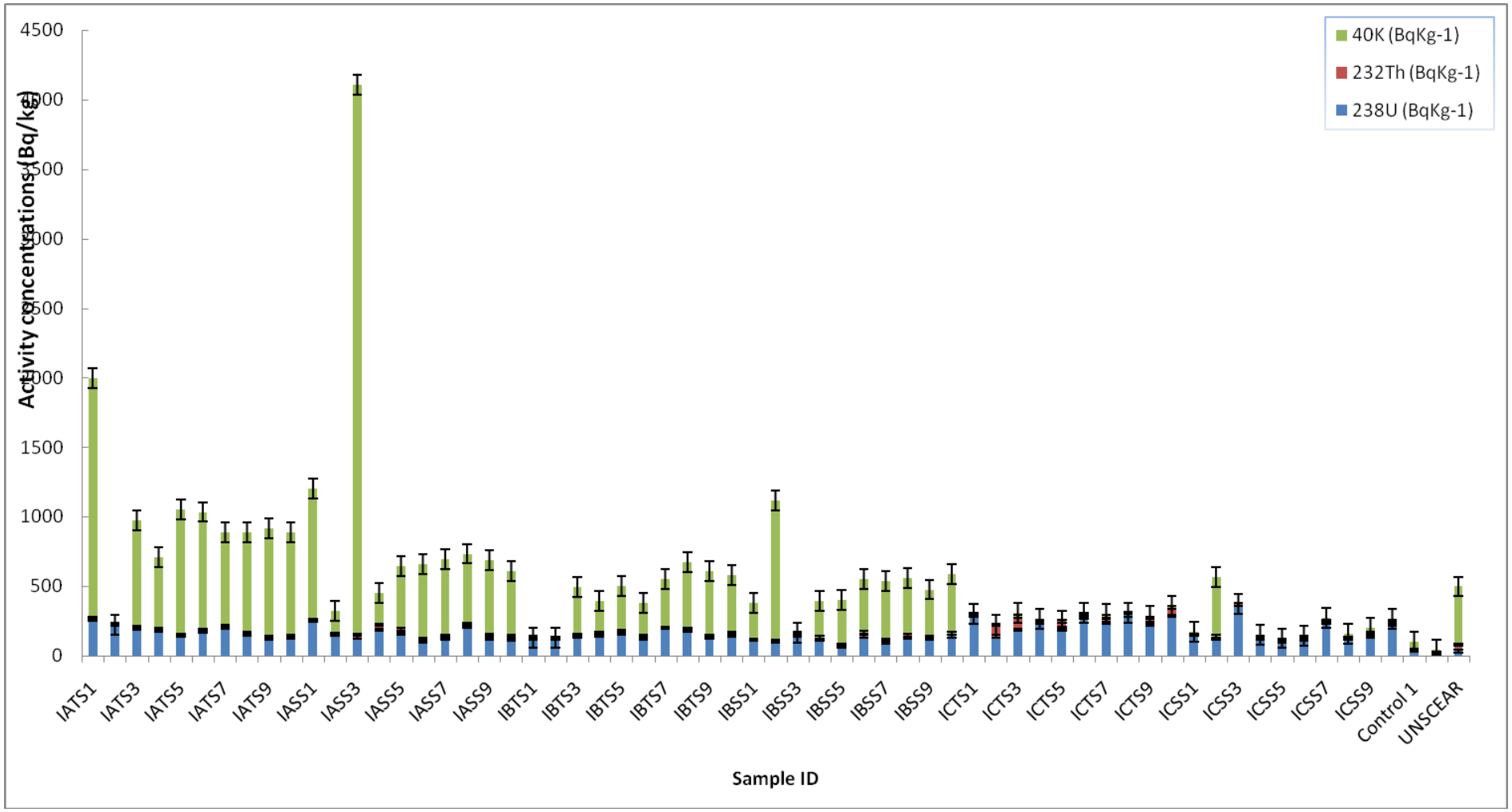

Fig. 2: Activity concentrations of radioisotopes ^{238}U, ^{232}Th and ^{40}K in the selected dumpsites and control soils.

323 The average absorbed dose rate (D_R) due to γ-radiation inhaled in air at 1 m above the ground surface
324 for the uniform distribution of the naturally occurring radioisotopes ^{238}U, ^{232}Th and ^{40}K for all
325 samples were calculated using equation based on the guidelines provided by (UNSCEAR, 2000)
326 (Table S1). The absorbed dose (D_R) ranged from 40.65 ± 10.6 - 215.95 ± 25.6 $nGyhr^{-1}$ with an
327 average value of 90.54 ± 14.9 $nGyhr^{-1}$ (Table 1). This estimated average value of D_R was higher than
328 the world average value of 57 $nGyhr^{-1}$(population weighted average) (UNSCEAR, 2000) (Fig. 3).
329 Radium equivalent activity (Ra_{eq}) introduced to define uniformity in the distribution with respect to
330 radiation exposure due to the naturally occurring radioisotopes in the soil samples (UNSCEAR,
331 2000). Ra_{eq} is the weighted sum of ^{238}U, ^{232}Th and ^{40}K based on the assumption that 370 Bq kg^{-1} of
332 ^{238}U, 259 $Bqkg^{-1}$ of ^{232}Th and 4810 $Bqkg^{-1}$ of ^{40}K gives the same γ-radiation dose rate (Straden,
333 1979). The maximum value of Ra_{eq} must be <370 $Bqkg^{-1}$ for the radiological effects to be
334 insignificant on the people living or working around the dumpsites i.e., scavengers or the nomadic
335 farmers. The value of Ra_{eq} obtained ranges from 84.9 ± 23.0 ↔ 420.30 ± 55.4 Bq kg^{-1} with an
336 average of 193.14 ± 32.3 $Bqkg^{-1}$ (Table 1). The values obtained for Ra_{eq} were lower than the world
337 average value of 370 Bq kg^{-1} except at four sampling points IATS1, IASS3, ICTS10 and ICSS3
338 (Ikoto topsoil and subsoil, Olisa topsoil and subsoil), (Fig. 3). The average value for Ra_{eq} were below
339 the recommended world average of 370 Bq kg^{-1}(UNSCEAR, 2000) in all the samples and meet the
340 recommended limit set by (OECD, 1979). The calculated outdoor and indoor AEDE values as shown
341 in Table 1 ranges from 49.88 ± 13 - 265.02±31.4 $\mu Svyr^{-1}$ and 199.5 ± 51.9 - 1060±126 $\mu Svyr^{-1}$ (Fig.
342 3) with an average value of 111.1 ± 18.3 $\mu Svyr^{-1}$ and 444.5 ± 73.3 $\mu Svyr^{-1}$ respectively. This
343 calculated average values for the outdoor and indoor AEDE were higher than the recommended limit
344 of 70 and 410 (UNSCEAR, 2000). These higher values for the AEDEs may be attributed to higher
345 ^{238}U and ^{40}K in the soils.

346 Annual genetically significant dose equivalent (AGDE), widely used to determine the genetic
347 significance of the yearly dose equivalent (Morsy et al., 2012) was calculated to range from 283.7 ±
348 71.4 - 1577 ± 155.6 $\mu Svyr^{-1}$, with an average value of 620.5 ± 101.2 $\mu Svyr^{-1}$ respectively. These
349 AGDE values obtained were higher than the worldwide average value of 1000 (UNSCEAR, 2000) at
350 four out of the sixty sampling points (6.7 %) and moderately high at five of the sampling points (8.3
351 %). The highest AGDE of 1577 ± 155.6 $\mu Svyr^{-1}$ values was obtained in IASS3 (Fig. 3).
352

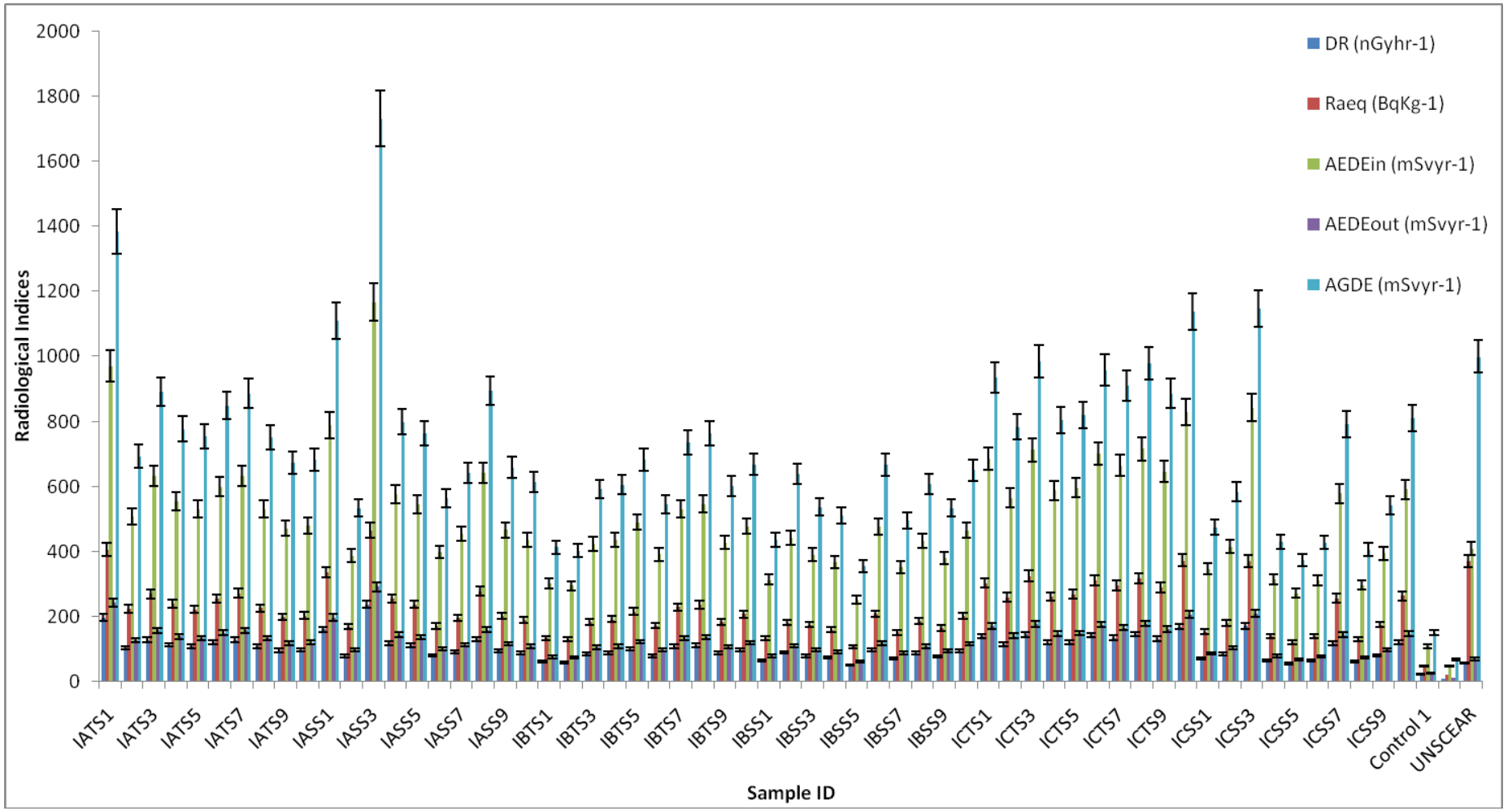

353

354 Fig. 3: Radiological parameters of the dumpsites soil and control samples

355

356 **3.2 Radiological and Health Hazard Indices**

357 The external radiation hazard index (H_{ext}), a globally used hazard index which reflects the external
358 exposure level due to γ-radiation in any environmental samples, was calculated for the samples. The
359 values obtained ranged from 0.23 ± 0.06 to 1.14 ± 0.12 (Table 1). The average value of 0.52 ± 0.10
360 obtained for H_{ext} in all the soil sampled was less than the acceptable limit of 1. All the samples had
361 H_{ext} value less than unity except for samples IATS1, IASS3, ICTS10 and ICSS3 which is the Ikoto
362 top and sub-soil and Olisa top and subsoil respectively (Fig. S1). The internal hazard (H_{int}) varied
363 from 0.36 ± 0.11 to 1.70 ± 0.30 with an average value of 0.91 ± 0.16. This value was higher than the
364 recommended value which must be ≤ 1. Hence, these areas may pose significant radiological risks to
365 the inhabitants owing to the harmful effects of ionizing radiation emanating from the dumpsites.
366 These calculated H_{int} values were above the recommended value in 47 % of the samples (28 sampling
367 points) (Fig. S1).
368 To further evaluate the radiation hazards associated with the dumpsite soil samples, another radiation
369 hazard index known as γ-radioactivity level index (Iγr)/γ-representative level index (RLI) was
370 determined. Based on (UNSCEAR, 2000) guidelines, for radiological effects to be considered
371 negligible, the values of each H_{ext}, H_{int} must be ≤ 1 and Iγr must be ≤ 0.5. The calculated value γ-ray
372 hazard index of the soil samples ranged from 0.36 ± 0.08 - 1.69 ± 0.17 with an average value of 0.68
373 ± 0.11, respectively. The calculated values of Iγr were higher than the recommended value of 0.5 in
374 all the sampling points except in IBTS2, IBSS1, ICSS5 and ICSS8 (Fig. S1) where the values were
375 below the recommended threshold. Therefore, caution should be taken in using the soils from these
376 dumpsites as bulk building materials because their γ-index values were higher than the upper limit set
377 by (UNSCEAR, 2000).
378 The dumpsite soil samples were also examined to evaluate whether they satisfy the dose criteria
379 when used as a building material. For this reason, the activity utilization index (AUI) was calculated.

The calculated values for AUI ranged from 0.58 ± 0.20 - 3.00 ± 0.36 with an average value of 1.54 ± 0.28 respectively (Table 1). The calculated values for AUI were higher than the recommended value/worldwide average value of ≤ 2 in nineteen out of the sixty samples analyzed (31.6 % of the sampling points) and moderately high in eighteen of the samples (30 %) (Fig. S1). The average value of AUI was moderately high in the samples. This shows that the present dumpsites soil samples cannot be used for safe construction of a building or agricultural purposes without adequate soil remediation or recontamination process.

3.3 Excessive Lifetime cancer risk (ELCR) and exposure rate (ER)

The outdoor excessive life cancer risk ($ELCR_{out}$) was calculated on the annual outdoor effective dose equivalent and the results were presented in Table 1. The outdoor excessive life cancer risk ($ELCR_{out}$) ranged from 175 ± 45.5 - 928 ± 94.6 with an average value of 388.9 ± 64.1 respectively (Table 1). $ELCR_{outdoor}$ values calculated were higher than the recommended limit of 290 (UNSCEAR, 2000) in about 88 % of the samples (Fig. S2). Consequently, the average value was higher than the world average value in all the dumpsites soil samples. This result shows that the lifetime cancer risk due to exposure using this dumpsite soils for 70 years maximum duration is high. Hence, the subsequent use of this dumpsite soil for building construction, agriculture or for soil remediation studies and other purposes should be discouraged.

The calculated rate of exposure (ER) of an individual and scavengers to these naturally occurring radioisotopes in the selected dumpsites was higher than the maximum limit in seven locations (IATS1, IASS1, IASS3, ICTS3, ICTS8, ICTS10 and ICSS3) and moderately high in three sampling points (ICTS6, ICTS7 and ICTS9) respectively (Fig. S2) (Table 1) (UNSCEAR, 2000). These results revealed that Ikoto and Olisa dumpsite has a higher ER value. Hence the people living near these dumpsites should be aware of the inherent effects of exposure to this harmful ionizing radiation emanating from these dumpsites on daily basis.

404

405 Table 2: Statistics summary of the potentially toxic metals (PTMs) (mg kg^{-1}) in the dumpsite soil

406 samples (n=60), control (n =2) and guidelines values

PTMs	Pb (mg kg^{-1})	Cd (mg kg^{-1})	Cr (mg kg^{-1})	Ni (mg kg^{-1})	Zn (mg kg^{-1})
Arithmetic Mean	22.35	17.95	20.83	19.02	75.88
Max.	41.82	29.21	34.87	31.12	142.54
Min.	11.14	8.14	11.43	9.23	23.76
Range	30.68	21.07	23.44	21.89	118.78
Median	20.15	18.06	20.26	19.14	67.06
SD	5.61	4.38	5.25	3.09	37.92
RSD or CV (%)	32.7	27.5	25.1	26.0	42.7
Kurtosis	0.06	-0.48	0.02	0.24	-1.04
Skewness	0.74	-0.03	0.11	0.11	0.48
SEM	0.94	0.64	0.67	0.64	4.19
ABV	11.39	6.95	39.59	7.34	13.55
SOGs	50	0.4	-	60	300
MAL (Austria)	100	5	100	100	300
MAL (Canada)	200	8	100	100	400
MAL (Poland)	100	3	100	100	300
MAL (Japan)	400	-	-	100	250
MAL (Germany)	500	2	200	100	300
MAL (Great Britain)	100	3	50	50	300
(DEP, Australia)[a]	300	3	50	60	200
(CCME, Canada)[b]	70	1.4	64	50	250

[a] DEP (Department of Environmental Protection) (2003).; [b]CCME (Canadian Council of Ministers of the Environment) (2003).

3.4 Potentially toxic metals (PTMs) in the dumpsite soils

The descriptive statistics of potentially toxic metals (PTMs) concentrations in the dumpsite soil samples and the corresponding background samples are presented in Table 2. The mean concentrations of Pb, Cd, Cr, Ni and Zn ranged from 11.14 - 41.82, 8.14 - 29.21, 11.43 – 34.12, 9.23 – 31.12 and 23.76 – 142.54 mg kg^{-1} with a mean value of 22.35, 17.95, 20.83, 19.02 and 75.88 mg kg^{-1} respectively (Fig. 4). Among the five studied PTMs, Zn, Pb, and Cr had the highest mean concentrations. Coefficient of variation which is a measure of relative dispersion within the concentrations of the PTMs defined as the ratio of the standard deviation to the mean concentration of the PTMs. The greater the CV, the greater the level of dispersion around the mean. If CV ≤ 20%, it shows low dispersion; if 21% < CV ≤ 50 %, it is referring to as moderate dispersion; 50% < CV ≤ 100% is regarded as high dispersion or variability; while CV value above 100% is considered as high dispersion or variability (Karim et al., 2015). The CV of the PTMs increased in the order of Zn (42.7) > Pb (32.7) > Cd (27.5) > Ni (26.0) > Cr (25.1) (Table 2). The CV for the five PTMs in this study indicated that the PTMS varied moderately with respect to the different samples. Kurtosis and skewness are two main measures of the degree of asymmetry in relation to normal distribution of variables (Liu et al., 2017). The PTMs were positively skewed towards lower concentrations except Cd, Pb, Cr and Ni showed a heavy tailed distribution with positive kurtosis and Cd and Zn shows a lightly tailed distribution with negative kurtosis. Moreover, the mean and maximum concentration of Cd among the PTMs measured exceeds the maximum allowable limit (MAL) for Cd in Austria, Canada, Poland, Japan, Germany and Great Britain (Table 2).

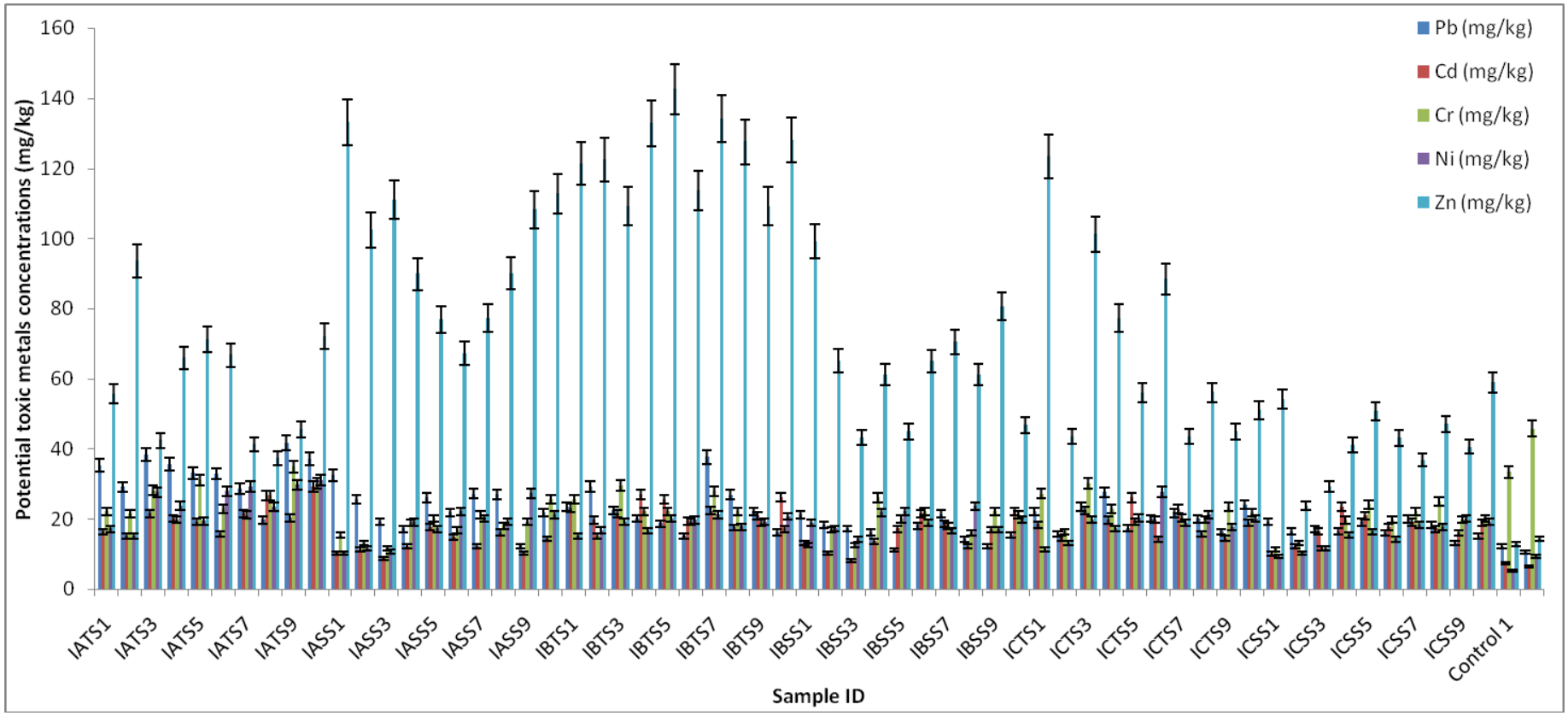

Fig. 4: PTMs distribution in the dumpsite soil and control samples

3.5 Spatial Distribution of PTMs and radioisotopes using MATLAB

The degree of activity concentrations of radioisotopes ^{238}U, ^{232}Th, ^{40}K and potentially toxic metals (PTMs) Pb, Cd, Cr, Ni and Zn in the three dumpsites are shown in Fig. 5. The concentrations are presented in three-dimensional distributions using MATLAB (Miao et al 2014), where the degree of concentrations indicated by the colour bar. As shown in the colour bar (Fig. 5), the trend of concentrations is upward with different concentration values ranging from 0 mg/kg to the higher concentration value (3500 mg/kg). The higher concentrations value of radioisotopes ^{238}U, ^{232}Th and ^{40}K in Fig. 5 (a), (b) and (c) are indicated by yellow, purple and red respectively, while those of PTMs are shown in Fig. 5 (d), (e),(f),(g), and (h) maintain the similar colour trend (pink) except the Fig. 5 (f) with a different control colour. This is because the concentrations of Cr among the PTMs in the control samples are higher than what is obtained in the three dumpsites soils. The concentration of the control ranged from 33.45 mg/kg - 45.72 mg/kg against the Cr value in the three dumpsites which ranged from 11.43 mg/kg to 27.21 mg/kg (Table 2).

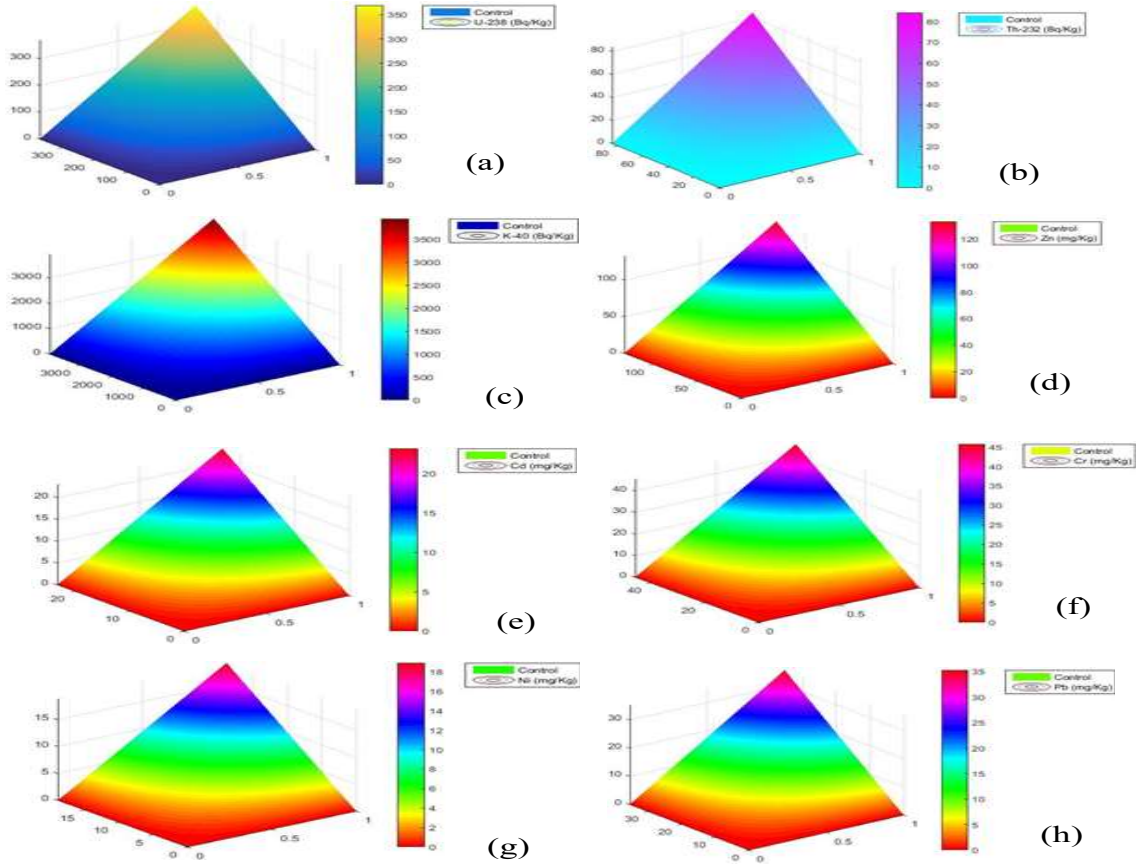

Fig. 5: Activity concentrations of radioisotopes (a) ^{238}U, (b) ^{232}Th, (c) ^{40}K, and PTMs (d) Pb, (e) Cd, (f) Cr, (g) Ni, and (h) Zn in the study area (the colours in the legends represent the corresponding concentration values of radioisotopes and PTMs in dumpsite and control soils).

3.6 Assessment of Pollution and Ecological Risk Indices of Potentially toxic metals (PTMs)

The potential toxic metals pollution and ecological risk assessment such as index of geo-accumulation (Igeo), contamination factor (CF), pollution loading index and potential ecological risk index (PERI) were used to evaluate the degree of PTMs pollution of the dumpsite soils (Table 3). The Igeo of the five PTMs in the dumpsites ranged from 1.93 - 2.50, 1.58 - 2.13, 2.48 - 2.96, 1.66 - 2.18 and 2.33 - 3.11 for Pb, Cd, Cr, Ni and Zn, respectively. Higher Igeo values were reported for Zn Cr and Pb (Table 3). Based on the index of geo-accumulation obtained, the dumpsite soil was moderately to strongly polluted with the PTMs. The estimated value of the contamination factor (CF)

458 revealed that the dumpsite soils was moderately to considerably contaminated with Pb (0.98 - 3.67),
459 Cr (1.00 - 3.06), Cd (0.72 - 2.57) and Ni (1.26 - 2.58), strongly contaminated with Zn (2.09 - 12.52)
460 respectively. The level of PLIs in the study sites varied from 0.40 - 5.29, indicating that selected
461 dumpsite showed low pollution for Pb, Cd, Ni and heavily polluted with Zn. The potential ecological
462 risk index (PERI) which represents the sensitivity of various microorganisms to toxic metals in the
463 area and indicate the risk of the hazardous metals in the soils (Islam et al., 2015) are as shown in
464 Table 3. The potential ecological risk index (PERI) of the five PTMs increases in the following order:
465 Cr < Zn < Ni < Pb < Cd (Table 3). The results showed that the dumpsites posed a greater ecological
466 risk through the PTMs to the biological communities in the study area.

467 **Table 3: Statistical summary of Igeo, CF, PLI and PERI**

Potentially toxic metals (PTMs)	Range of PTMs concentrations ($mgkg^{-1}$)	Igeo	CF	PLI	PERI
Pb	11.14 - 41.82	1.93 - 2.50	0.98 - 3.67	≤ 1.9	4.90 - 18.4
Cd	8.14 - 29.21	1.58 - 2.13	0.72 - 2.57	≤ 1.9	21.5 - 77.0
Cr	11.43 - 34.87	2.48 - 2.96	1.00 - 3.06	≤ 0.4	2.01 - 6.13
Ni	9.23 - 31.12	1.66 - 2.18	0.81 - 2.73	≤ 1.8	4.05 - 13.7
Zn	23.76 - 142.54	2.33 - 3.11	2.09 - 12.52	≤ 5.29	2.09 - 12.5

468

469 **3.8 Potential Human risk assessment of PTMs - Carcinogenic and Non-carcinogenic risk**

470 The human health risk assessment which was calculated based on the concentrations of PTMs in the
471 dumpsite soils are shown in Table 4 and in supplementary materials (Table S3a and S3b). The mean
472 non-carcinogenic risk (HQ) of PTMs through the three exposure pathways for children and adults in
473 the dumpsite soil are in the order of $HQ_{dermal} > HQ_{ingestion} > HQ_{inhalation}$ respectively (Table S3b).
474 Dermal contact contributed from about 69 % of the THI with the highest obtained for Zinc. These
475 results are in consistent with previous studies (Jamal et al., 2018; Gbadamosi et al., 2018a; Zhou et
476 al., 2020). The carcinogenic risk (CR) for the three carcinogenic metals for children and adults were
477 in the order: Cr (9.61E-04) > Cd (1.24E-04) > Ni (1.76E-05) and Cr (6.92E-05) > Cd (2.05E-05) > Ni

478 (3.75E-07) (Table 4). More so, the total carcinogenic risk (TCR) for children with respect to the three
479 exposure pathways is about 1220 times greater than for adults. This revealed that the children are
480 likely to suffer more carcinogenic risk on exposure to the PTMs in the dumpsite soils samples via
481 multiple exposure routes. These values obtained for children and adults were higher than the
482 acceptable limit (1E-06). This showed that the dumpsite soil samples posed greater carcinogenic
483 health risk for children and adults. Overall, the non-carcinogenic risks of the five PTMs were all <1,
484 which shows that there would be no non-carcinogenic risk from the concomitant effect of the five
485 PTMs in the study areas.
486

Table 4: potency factors, carcinogenic and non-carcinogenic risks of the heavy metals in the dumpsite soil to children and adults

PTMs	EPCsoil		Children		Adults	
	($mg.kg^{-1}$)	PF $(mg/kg\text{-}day)^{-1}$	THI	Cancer risk (CR)	THI	Cancer risk (CR)
Pb	22.35		8.29E-02		1.33E-02	
Cd	17.95	8.40E-01	2.91E-01	1.24E-04	1.49E-01	6.92E-05
Cr	20.83	6.30E+00	1.04E-01	9.61E-04	4.05E-02	2.05E-05
Ni	19.02	4.20E+01	1.23E-02	1.76E-05	1.86E-03	3.75E-07
Zn	75.88		2.84E-01		5.38E-01	
∑HI			7.74E-01		7.42E-01	
∑CR				1.10E-03		9.01E-05

Table 5: The observed absorption band and their corresponding minerals identified from FTIR spectra

SI. No	Range of observed wave number (cm^{-1})	Sample ID	Minerals
1.	696.52 - 1059.14	IATS1 - IATS10	Quartz
	1692 - 1868.3	IATS1 - IATS10	Quartz
	669.96 - 1008.45	IASS1 - IASS10	Quartz
	753.52 - 1003.52	IBTS1 - IBTS10	Quartz
	756.60 - 1034.34	IBSS1 - IBSS10	Quartz
2.	911.39 - 1004.29	ICTS1 - ICTS10	Kaolinite
	3621.75 - 3695	ICTS1 - ICTS10	Kaolinite
	3426 - 3646.3	ICSS1 - ICSS10	Kaolinite
3.	2003.5 - 2301	IATS1 - IATS10	Organic carbon
	2859.8 - 2916.9	IATS1 - IATS10	Organic carbon
	2915.9 - 2921.6	ICTS1 - ICTS10	Organic carbon
4.	3612 - 3896	IBTS1 - IBTS10	Carbonates

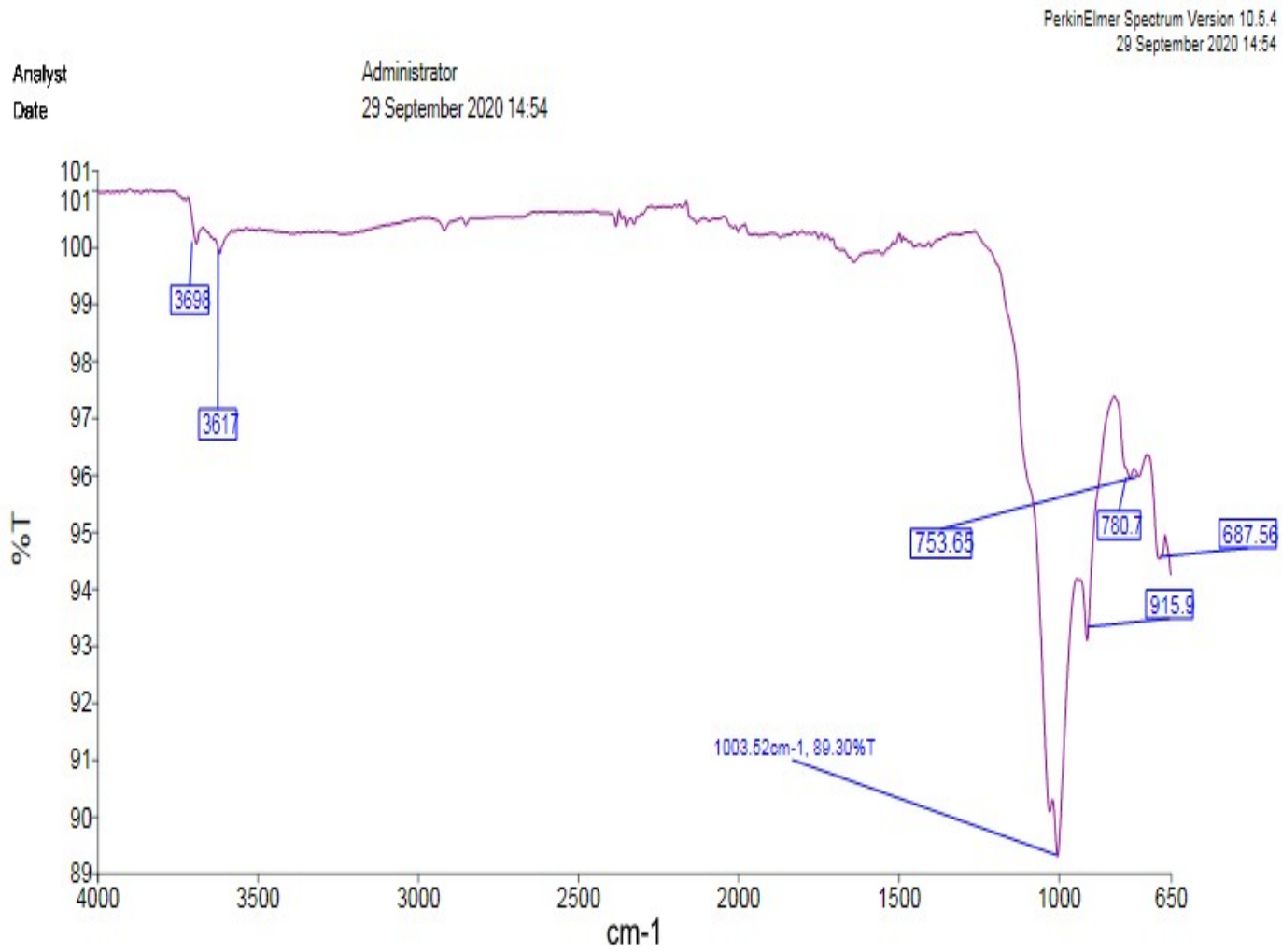

Fig. 6: Fourier-transform infrared spectrometer (FTIR) spectrum for sample ID IBTS2

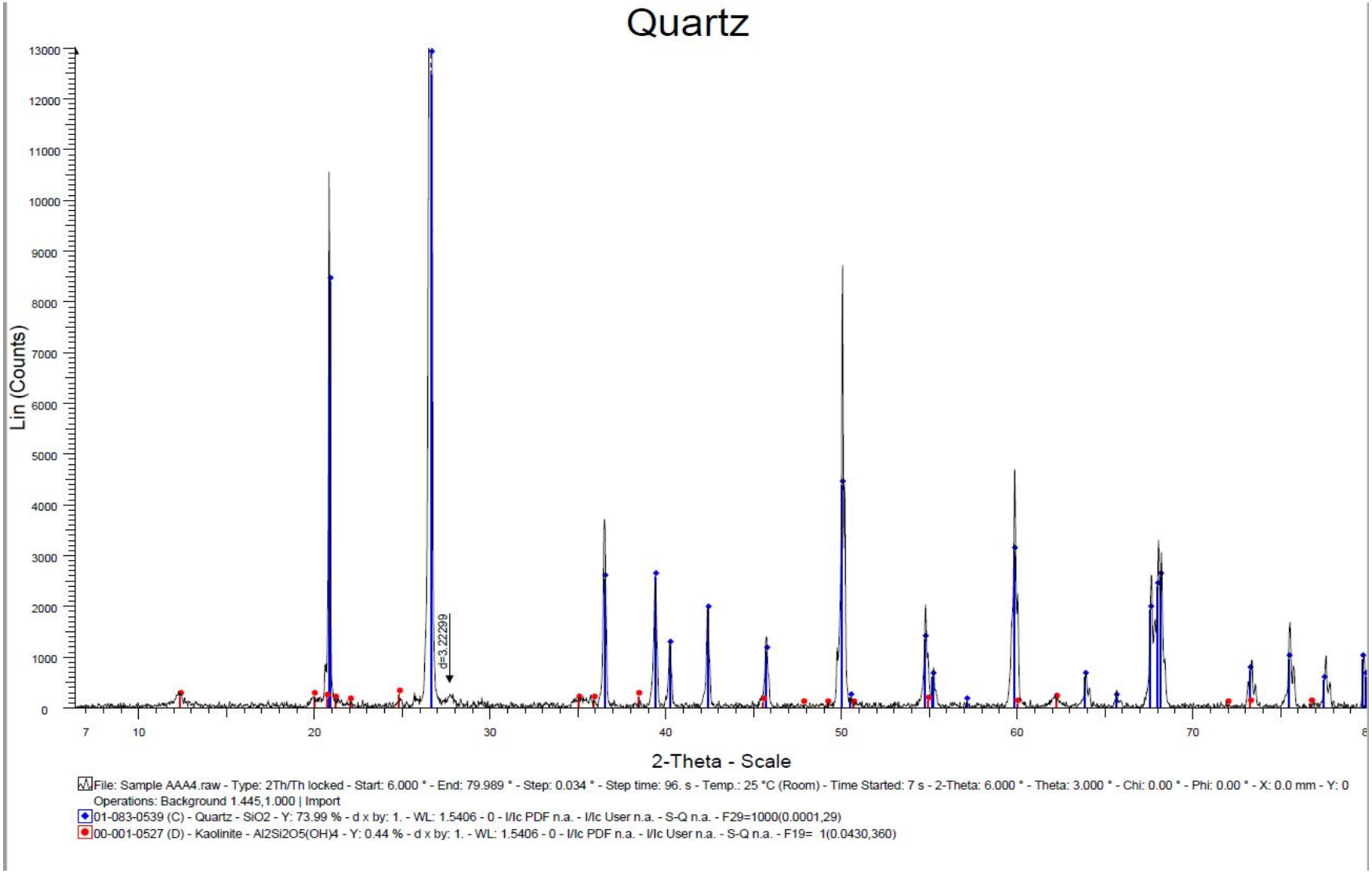

Fig. 7: XRD pattern of sample ID IATS3

3.7 Mineralogical characterization (FTIR and XRD)

3.7.1 FTIR analysis

The soil samples were subjected to Fourier transform infrared (FTIR) spectrometer complemented by x-ray diffraction (XRD) to assess the mineralogical composition of the soil samples from the study area. The FTIR absorption bands for the different soil samples with their corresponding minerals are presented in Table 5. The FTIR results showed that among the four minerals identified, quartz and kaolinite were the major minerals based on their peak intensities in all the samples (Fig. 7). Quartz is abundant mineral in soil due its chemical structure and hardness, it gives characteristics Si-O symmetrical stretching vibration at 778 - 796 cm^{-1}, Si-O asymmetrical bending vibrational frequency at 462 - 694 cm^{-1} and Si-O asymmetrical stretching vibration at 1082 - 1162 cm^{-1} because of low Al to Si substitution (Paramasivam et al., 2019). The chemical weathering of Feldspars produced Kaolinite ($Al_2Si_2O_5(OH)_4$) which is a clay mineral. The presence Kaolinite is indicated with a vibrational frequency in the range 3621.75 - 3695 cm^{-1} and 911.39 - 1004.29 cm^{-1}. The appearance of peaks in the range 2859.8 - 2916.9 $cm^{-1}$and 2915.9 - 2921.6 cm^{-1} indicated the presence of organic carbon and a sharp peak between 3612 - 3896 cm^{-1} revealed the presence of carbonate (Fig. 6).

3.7.2 XRD analysis

XRD analysis was applied to complement the FTIR results. The diffraction patterns are obtained through phase identification by comparing the diffraction pattern with a JCPDS database. The minerals identified were quartz and kaolinite (Fig. 7). Quartz showed a high peak intensity in all the samples analyzed. As a result of disordered (loss of crystalline nature) of the respective minerals, some minerals did not show in the XRD results as compared to the results obtained from the FTIR (Fig. 6). Nevertheless, the XRD results also shows that quartz and kaolinite were the major minerals in the soil samples with high peak intensities (Fig. 7) and this is in tandem to FTIR results.

548 **3.9 Pollution source identification and apportionment using multivariate statistical analysis**

549 Multivariate statistical analysis such as Pearson's correlation analysis (CA), principal component
550 analysis (PCA) and hierarchical cluster analysis (HCA) were employed to evaluate the
551 interrelationship among the PTMs, radioisotopes and its associated radiological parameters in
552 dumpsites soil characteristics due to its usefulness as a dimension reduction technique widely applied
553 in environmental monitoring studies without losing much information (Gbadamosi et al., 2018a). The
554 statistical analyses were carried out using the commercial statistics package IBM SPSS statistics
555 (version 26).

556 **3.9.1 Pollution sources identification and apportionment using principal component analysis**
557 **(PCA)**

558 Principal component analysis (PCA) was carried out to apportion the potentially toxic metals
559 (PTMs), radioisotopes and their associated radiological parameters pollution sources in these study
560 areas. This was performed based on varimax orthogonal rotation and eigenvalue > 1 after Kaiser-
561 meyer Olkin Normalization measuring of adequacy and Bartlett's test significant value for all the
562 variables. Potentially toxic metals and radioisotopes and their associated radiological parameters
563 originating from similar source(s) were always grouped with strong loadings. The results obtained
564 showed that there is an initial dimensional reduction of all the dataset to four components which
565 explained 86.8 % of the data variation (Table 6). The first principal component (PC-1) explained 61.7
566 % of the total variance and was heavily loaded by ^{238}U and all the radiological parameters and health
567 hazard parameters (0.814-0.998) (Table 6, Fig. 8). This confirmed that the radiological and health
568 hazards parameters were mainly determined by the level of ^{238}U in the samples. The second principal
569 component (PC-2) was dominated by the toxic metals Ni, Cd, Pb and Cr with high loadings values of
570 0.768, 0.724, 0.632 and 0.577 respectively (Table 6). This component which accounted for 10.0% of
571 the total variance determined and is mainly attributed to anthropogenic sources of the toxic metals in
572 the dumpsites. This component could be defined as a combination of natural and anthropogenic

component. The third and fourth principal components (PC-3 and PC-4) accounted for 8.8 % and 6.3 % of the total variance explained. PC-3 loaded heavily on ^{40}K (0.874) while PC-4 loaded heavily by Zn and moderately negative with ^{232}Th respectively (Table 6). From the results and values obtained from pollution assessment, it clearly revealed that PC-1 and PC-2 represent mixed natural, anthropogenic and lithogenic sources mainly from aggregation of lead-containing materials in the waste on the dumpsites, vehicular emission, industrial discharges and atmospheric depositions (Kong et al., 2014; Li et al., 2018), while PC-3 and PC-4 are mainly related to anthropogenic activities resulting from agronomic used of potassium-rich fertilizer and waste discharge from nearby industries into the dumpsites.

Table 6: Principal component analysis (after varimax rotation) showing contribution of statistically dominant variables measures in this study

	Principle loading factors				Communalities
Variables	1	2	3	4	
Hext	**0.998**	0.054	0.022	0.030	0.999
Raeq ($BqKg^{-1}$)	**0.998**	0.054	0.022	0.030	0.999
AEDEin ($mSvyr^{-1}$)	**0.991**	0.051	0.112	0.045	0.999
D_R ($nGyhr^{-1}$)	**0.991**	0.051	0.112	0.045	0.999
ELCRout	**0.991**	0.051	0.112	0.045	0.999
AEDEout ($mSvyr^{-1}$)	**0.991**	0.051	0.112	0.045	0.999
ER (μRhr^{-1})	**0.990**	0.051	0.118	0.032	0.998
Iγr	**0.986**	0.050	0.147	0.032	0.997
AGDE ($mSvyr^{-1}$)	**0.982**	0.049	0.169	0.045	0.998
Hint	**0.963**	0.060	-0.182	0.086	0.971
AUI	**0.886**	0.062	-0.439	0.008	0.981
^{238}U ($BqKg^{-1}$)	**0.814**	0.061	-0.416	0.145	0.860
Ni (mg/kg)	0.092	**0.768**	0.000	-0.031	0.599
Cd (mg/kg)	0.069	**0.724**	-0.363	0.186	0.695
Pb (mg/kg)	0.282	**0.632**	0.280	0.311	0.654
Cr (mg/kg)	-0.300	**0.577**	0.120	-0.418	0.611

^{40}K (BqKg^{-1})	0.411	-0.004	**0.874**	0.069	0.939
Zn (mg/kg)	0.100	0.115	0.030	**0.818**	0.693
^{232}Th (BqKg^{-1})	0.380	0.023	-0.400	**-0.409**	0.472
Eigen-value	11.833	1.863	1.699	1.068	-
% of variance explained	61.7	10.0	8.8	6.3	-
Cumulative (%)	61.7	71.7	80.5	86.8	-

584

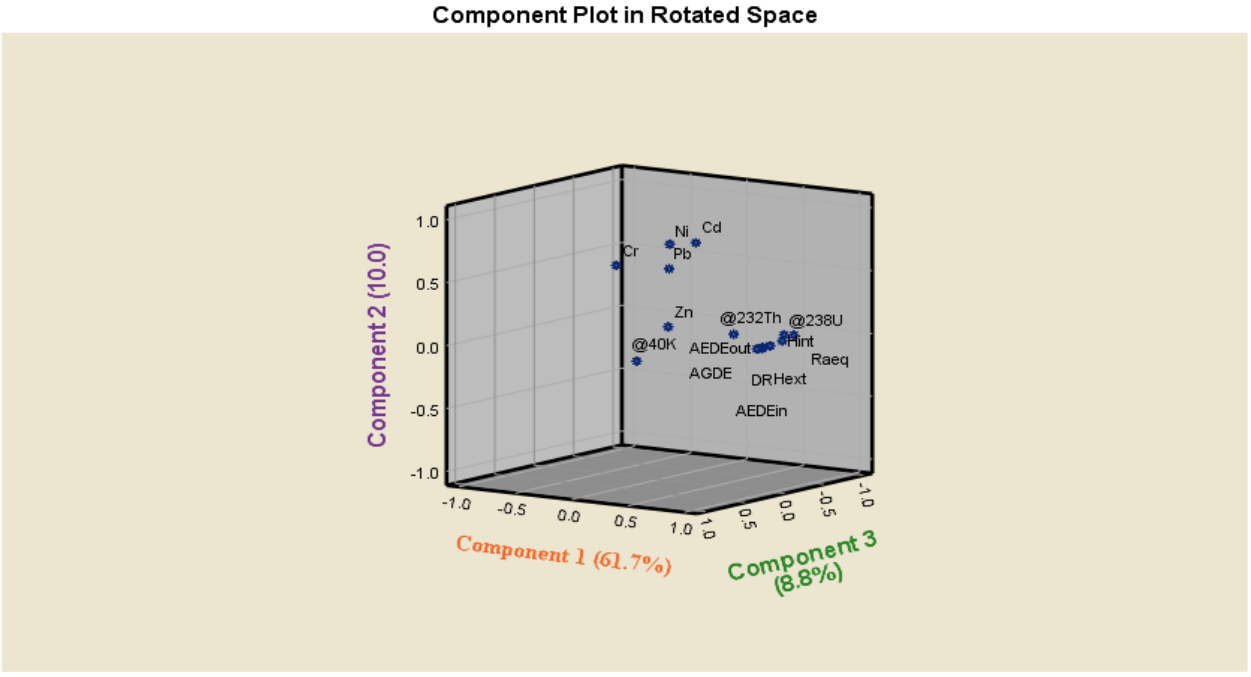

585

586 Fig. 8: Graphical representation of components

587 **3.9.2 Hierarchical cluster analysis (HCA)**

588 Hierarchical cluster analysis (HCA) is a multivariate statistical analysis commonly used to quantify
589 the similarity of the variables and analyze the effect of the factor on the samples using a variance
590 approach to define the distance between the clusters (Jiang et al., 2015). In HCA, the average linkage
591 method along with coefficient distance was used with an explicit dendrogram (Fig S3). In the
592 dendrogram shown, the potentially toxic metals (PTMs), radioisotopes and their associated
593 radiological parameters were grouped into four statistically significant clusters. Cluster-I consisted of

(all the heavy metals, H_{ext}-Iγr-H_{int}-AUI-^{232}Th-D_R-$AEDE_{out}$-^{238}U-Ra_{eq}). These are considered to originated from mixed natural, anthropogenic and lithogenic sources. However, the anthropogenic influences are of greater impact. Cluster-II is made up of (ER-$ELCR_{out}$ and $AEDE_{in}$). Cluster-III consisted of AGDE while Cluster-IV consisted of ^{40}K. Cluster-II and cluster-III have a minor similarity and a major similarity with Cluster-IV (Fig. S3). This shows that Cluster-IV (^{40}K) was the main determinant of the radiological parameters such as ER, ELCRout, AEDE and AGDE showed in Cluster-II and Cluster-III.

3.9.3 Pearson's correlation coefficients analysis

Pearson's correlation matrix (PCM) was carried out in order to establish the strength of association and direction of the linear relationship between the variables through the calculation of the linear Pearson product moment correlation coefficient (r).

A correlation analysis between radioisotopes and their associated radiological parameters, potential toxic metals in the sampling areas clearly revealed a strong positive correlation between ^{238}U and the estimated associated radiological parameters at 0.01 level of significance ($P \leq 0.01$) (2-tailed) (Table S5). A moderate correlation occurs between ^{40}K and the estimated radiological parameters. This shows that ^{238}U activity concentration is the main factor responsible for the radiological parameters determined in the samples. A weak correlation existed between ^{232}Th with other radioisotopes. A moderate positive correlation existed between Pb and Ni (0.374), Cd and Ni (0.470) at 0.01 level of significance ($p \leq 0.01$) (Table S5). All other PTMs correlated weakly with other radioisotopes and their associated radiological parameters in this study. This correlation results vividly revealed that the calculated radiological parameters correlated highly in the study, due to high concentration of ^{238}U and ^{40}K in the dumpsites soil samples, which can be attributed to their common anthropogenic sources of pollution through extensive fertilizer application and radioactive materials in the deposited waste.

3.10 Spatial distribution of radioisotopes

The results obtained for the activity ratio for ^{238}U:^{232}Th activity concentrations in the dumpsite soils samples showed that ^{238}Th activity concentrations were about 4 times higher than the ^{232}Th activity concentrations in all the soil samples. The activity concentration of ^{40}K is about 42 times and 11 times higher than the ^{232}Th and ^{238}U in the soil samples. The ratio $^{238}U/^{232}Th$ ratio (Table S6) is higher than the world's average value of unity in 92 % of the samples (fifty-five sampling points). The ratio of ^{238}U: ^{232}Th, ^{238}U: ^{40}K and ^{232}Th: ^{40}K suggests that the soil samples from a certain area had higher or lower ^{238}U, ^{232}Th and ^{40}K activity concentration to be economically suitable for extraction. ^{40}K and ^{238}U activity concentrations were higher in all the samples which may be due to (i) the presence and aggregation of clinical or medical wastes containing radioactive materials (uranium) in the dumpsites and extensive use of potassium rich fertilizer like phosphate in the soils. The sum and range of the individual activity ratio of the radioisotopes used for the box-plot in Fig. S4, shows that for $^{238}U/^{232}Th$, $^{238}U/^{40}K$ and $^{232}Th/^{40}K$ the range of the activity ratios are 1.65 - 244.6, 0.03 - 25 and 0.002 - 5.19 respectively (Fig. S4). This shows that the activity ratio for $^{238}U/^{232}Th$ were higher than the stipulated range of 0.7 - 0.4 (Mitchell et al., 2002; ICRP, 1976) and for some sampling sites, $^{232}Th/^{40}K$ also recorded higher values (Table S6). This could indicate the possibility of ^{238}U extraction from the study areas.

4 Conclusion

The activity concentrations of the radioisotopes and their associated radiological parameters, pollution and health risk assessment of the PTMs from the selected dumpsites in Ijebu-Ode were evaluated. The mean activity concentrations of the radioisotopes in the dumpsite soil samples were of the order; $^{40}K > ^{238}U > ^{232}Th$. The total and average activity concentrations of the radioisotopes^{238}U and ^{40}K were higher than the reported global average values. The dumpsites in these locations are hazardous based on the values of the average and maximum radiological and health parameters such

642 D_R, Ra_{eq}, H_{ext}, H_{int}, I_{yr}, ER, $AEDE_{indoor}$, $AEDE_{outdoor}$ and $ELCR_{oudoor}$ which were higher than the world
643 average values in most of the sampling points. The mean and maximum concentrations of the PTMs
644 were below the maximum acceptable limit (MAL) for the countries considered except Cd which has a
645 higher than the MAL in all the countries. The pollution and ecological risk assessment showed that
646 the selected dumpsites are moderately-strongly polluted with the metals and that the dumpsites could
647 pose great ecological risks to the biomes. The results of the health risk assessment model revealed
648 that the carcinogenic risk for children and adults with CR values of the three carcinogenic metals (Cr,
649 Cd and Ni) higher than the acceptable range ($1x10^{-6} \leftrightarrow 1x10^{-4}$). Mineralogical composition of the soils
650 was obtained from FTIR and confirmed through XRD suggest that the major minerals are quartz and
651 kaolinite with high peak intensities. Multivariate statistical analysis applied to attributes the sources
652 of radioisotopes and potentially toxic metals (PTMs) established an interdependent relationship
653 between the variables. This study therefore comprehensively evaluated and apportioned the PTMs
654 and radioisotopes pollution sources, human exposure risk assessment to the toxic metals from the
655 selected dumpsites and will serve as a reliable baseline data for future monitoring of the study areas
656 and areas of similar geology and environmental usage. It also provides useful information for the
657 Federal and State Ministry of Environment on waste management with respect to the continuous
658 deleterious emissions from waste dumpsites to the surrounding environment and likely contamination
659 of proximate surface and ground waters.

660 **Conflict of interest**

661 The authors declare no conflict of interest.

662

663 **Acknowledgements**

664 Authors wish to express appreciations Tai Solarin University of Education (TETFUND-IBR-Team 6)
665 grant and Babcock University for providing the financial support through Babcock University

Research Grant No: BU/RIIC/2018/016 to support this project. The authors also acknowledge the technical support received from Mrs Owoade and Mr Olubunmi Emmanuel Tope of the National Institute of Radiation and Protection, University of Ibadan, Ibadan during the analysis. All anonymous reviewers of this manuscript are well appreciated by the authors.

References

Ademola, J.A., Hammed, O.S., Adejumobi, C.A. 2008. Radioactivity and dose assessment of marble samples from Igbeti Mines, Nigeria*, Radiation Protection Dosimetry.* 132: 94-97.

Adeyemi, B. 2011. Waste Management in Contemporary Nigeria: The Abuja Example. *International Journal of Politics and Good Governance (2).*

Berry, I.G., 1974. Selected Powder Diffraction Data for Mineralogy, JCPDS, Swanthmore, PA, USA (1974)

Bourliva, A., Kantiranis, N., Papadopoulou, L., Aidona, E., Christophoridis, C., Kollias, P., Fytianos, K. 2018. Seasonal and spatial variations of magnetic susceptibility and potentially toxic elements (PTEs) in road dusts of Thessaloniki city, Greece: A one-year monitoring period. Science of the Total Environment, 639, 417–427. doi:10.1016/j.scitotenv.2018.05.170

CCME, Canadian Council of Ministers of the Environment (2003). Canadian Environmental Quality Guidelines.

Chakravarty, M., Patgiri, A.D.2009. Metal pollution assessment in sediments of the Dikrong River, NE India. J. Hum. Ecol. 27 (1), 63–67.

DEP (Department of Environmental Protection). 2003. Assessment Levels for Soil, Sediment and Water Contaminated Sites Management Series Perth's, Australia. www.environ.wa.gov.au/.

El-Amier, Yasser A., Elnaggar, Abdelhamid A., Muhammad, El-Alfy, A. 2017. Evaluation and

689 mapping spatial distribution of bottom sediment heavy metal contamination in Burullus Lake,
690 Egypt. Egyp. J. Basic Appl. Sci. 4, 56–66.
691 Fouzey, H.K., Yousif, M.Z., Asim, A.M., Amer, A.S. 2013. Study the radiological assessment for
692 Italian radioisotopes production laboratory (IPRL) (Tuwaitha-Iraq), *Journal of al-Nahrain*
693 *University*, 16:101-105.
694 Gabarrón, M.., Faz, A., Acosta, J. A. 2017. Soil or Dust for Health Risk Assessment Studies in Urban
695 Environment. Archives of Environmental Contamination and Toxicology, 73(3), 442-455.
696 http://doi.org/10.1007/s00244-017-0413-x.
697 Gbadamosi, M. R., Banjoko, O. O., Abudu, K. A., Ogunbanjo, O. O., & Ogunneye, A. L. 2017.
698 Radiometric evaluation of excessive lifetime cancer probability due to naturally occurring
699 radionuclides in wastes dumpsites soils in Agbara , Southwest, Nigeria, 24: 315–324.
700 Gbadamosi, M.R., Afolabi, T. A., Ogunneye, A. L., Ogunbanjo, O.O., Omotola. E.O., Kadiri, T.M.,
701 Akinsipo, O.B., Jegede, D.O. 2018a. Distribution of Radionuclides and Heavy Metals in the
702 Bituminous Sand Deposit in Ogun State , Nigeria – A multi-dimensional pollution, health and
703 radiological risk assessment. *Journal of Geochemical Exploration,* 190: 187–99.
704 doi:10.1016/j.gexplo.2018.03.006.
705 Gbadamosi, M.R., Afolabi, T.A., Banjoko, O.O., Ogunneye, A.L., Abudu, K.A., Ogunbanjo, O.O.,
706 Jegede, D.O. 2018b. Spatial distribution and lifetime cancer risk due to naturally occurring
707 radionuclides in soils around tar-sand deposit area of Ogun State, southwest Nigeria.
708 Chemosphere, 193: 1036-1048.
709 Hua, L., Yang, X., Liu, Y., Tan, X., & Yang, Y. 2018. Spatial Distributions, Pollution Assessment ,
710 and Qualified Source Apportionment of Soil Heavy Metals in a Typical Mineral Mining City
711 in China. Sustainability, 10:3115, http://doi.org/10.3390/su10093115.
712 ICRP, 1976. Recommendations of ICRP Publication 26. Oxford: Pergamon. International
713 Commission on Radiological Protection.

714 Ikporukpo, C. O. 2018. Journal of Geography and Regional Planning Urbanization and the
715 environment: The debate and evidence from two new cities in Nigeria, 11(5), 61–79.
716 https://doi.org/10.5897/JGRP2018.0681
717 Islam, M.S., Ahmed, M.K., Habibullah-Al-Mamun, M., Hoque, M.F. 2015. Preliminary assessment
718 of heavy metal contamination in surface sediments from a river in Bangladesh. Environ. Earth
719 Sci. 73, 1837–1848.
720 Jamal, A., Delavar, M. A., Naderi, A., Nourieh, N., Medi, B., &Mahvi, A. H. 2018. Human and
721 Ecological Risk Assessment : An International Distribution and health risk assessment of
722 heavy metals in soil surrounding a lead and zinc smelting plant in Zanjan , Iran. *Human and*
723 *Ecological Risk Assessment*, *0*(0), 1–16. http://doi.org/10.1080/10807039.2018.1460191.
724 Jiang, Y., Guo, H., Jia, Y., Cao, Y., & Hu, C. 2015. Chemie der Erde Principal component analysis
725 and hierarchical cluster analyses of arsenic groundwater geochemistry in the Hetao basin ,
726 Inner Mongolia. *Chemie Der Erde - Geochemistry*, *75*(2), 197–205.
727 http://doi.org/10.1016/j.chemer.2014.12.002
728 Jibiri, N.N., Isinkaye, M.O., Momoh, H.A. 2014. Assessment of radiation exposure levels at Alaba e-
729 waste dumpsite in comparison with Municipal waste dumpsite in South-west Nigeria. *Journal*
730 *of radiation research and Applied Science* 7: 536-541.
731 Karim, Z., Qureshi, B.A.L., Mumtaz, M., 2015. Geochemical baseline determination andpollution
732 assessment of heavy metals in urban soils of Karachi, Pakistan. Ecol. Indic. 48, 358–364.
733 Kong, X.L., Cao, J., Tang, R.Y., Zhang, S.Q., Dong, F. 2014. Pollution of intensively managed
734 greenhouse soils by nutrients and heavy metals in the Yellow River Irrigation Region,
735 Northwest China. Environ. Monit. Assess. 186, 7719–7731.
736 Li, F., Zhang, J., Cao, T., Li, S., Chen, Y., and Liang, X. 2018. Human Health Risk Assessment of

737 Toxic Elements in Farmland Topsoil with Source Identification in Jilin Province, China.
738 International Journal of Environmental Research and Public Health, 15:1040,
739 doi:10.3390/ijerph15051040.
740 Liu, X., Song, Q., Tang, Y., Li, W., Xu, J., Wu, J., Wang, F., Brookes, P.C. 2013. Human health
741 risk assessment of heavy metals in soil-vegetable system: a multi-medium analysis. Sci. Total
742 Environ. 463-464, 530–540.
743 Liu, H., Zhang, Y., Zhou, X., You, X., Shi, Y., Xu, J. 2017. Source identification and spatial
744 distribution of heavy metals in tobacco-growing soils in Shandong province of China with
745 multivariate and geostatistical analysis. Environ Sci Pollut Res 24(6):5964–
746 5975. https://doi.org/10.1007/s11356-016-8229-1.
747 Mamut, A., Eziz, M., Mohammad, A., Anayit, M., 2017. The spatial distribution, contamination, and
748 ecological risk assessment of heavy metals of farmland soils in Karashahar–Baghrash oasis,
749 northwest China. Hum. Ecol. Risk Assess. An Int. J. 23, 1300–1314.
750 Men, C.; Liu, R.; Xu, F.; Wang, Q.; Guo, L.; Shen, Z. 2018. Pollution characteristics, risk
751 assessment, and source apportionment of heavy metals in road dust in Beijing, China. Sci.
752 Total Environ., 612, 138–147.
753 Miao, Y., Ji,X., Wei, W., Wen, W. 2014. Analysis of Heavy Metal Pollution in Urban Topsoil.
754 Information Technology Journal, 13(9):1577-1590
755 Mitchell, G., Mihalynuk, L., Heaman, L.M. 2002. Age of mineralized porphyry at the log-tung
756 deposit W-Mo-Bi-Be (Beryl, Aquamarine), Northwest BC, British Columbia Geological
757 Survey. Geological Fieldwork, 1:35-40.
758 Morsy, Z. El-Wahab Magda Abd, El-Faramawy Nabil. 2012. Determination of natural radioactive
759 elements in Abo Zaabal, Egypt by means of Gamma Spectroscopy, Ann. Nucl. Energy, 44:8-
760 11.

761 Njoroge, G.K.2007. Environmental pollution and impacts on public health: Implications of the
762 Dandora municipal dumping site in Nairobi, Kenya". *Report* summary by Njoroge G.Kimani,
763 in cooperation with United Nations Environmental Programme and the St.John catholic
764 church, Korogocho.

765 Nton, M.E., Ikhane, P.R., Tijani, M.N. 2009. Aspect of Rock-Eval Studies of the Maastrichtian-
766 Eocene Sediments from Subsurface, in the Eastern Dahomey Basin Southwestern Nigeria.
767 European Journal of Scientific Research, 25(3), 417-427

768 Nyles, C.B., Ray, R.N. 1999. The nature and properties of soils.12th Ed. United States of America,
769 pp. 743- 785.

770 OECD, 1979. Organization for Economic Cooperation and Development, Exposure to radiation from
771 the natural radioactivity in building materials. Report by a Group of Experts, Nuclear Energy
772 Agency, Paris, France,

773 Ogunbanjo, O., Onawunmi, O., Gbadamosi, M., Ogunlana, A., Anselm, O. 2016. Chemical
774 speciation of some heavy metals and human health risk assessment in soil around two
775 municipal dumpsites in Sagamu, Ogun state, Nigeria. Chem. Speciat. Bioavailab. 28 (1–4),
776 142–151.

777 Ojoawo, S., Agbede, O., Sangodoyin, A. 2011. On the Physical Composition of Solid Wastes in
778 Selected Dumpsites of Ogbomoso land, South-Western Nigeria*, Journal of Water Resource*
779 *and Protection.* 3: 661-666.

780 Piccolo, A., Mbagwu, J.S.C. 1997. ExogenuosHumic. Substances as conditions for the rehabilitation
781 of degraded soil agro Foods Industry Hi-Tech., 21-28.

782 Ramasamy, V., Sundarrajan, M., Paramasivam, K., Meenakshisundaram, V., Suresh, G. 2013.

783 Assessment of spatial distribution and radiological hazardous nature of radionuclides in high
784 background radiation area , Kerala , India. *Applied Radiation and Isotopes*, *73*, 21–31.
785 http://doi.org/10.1016/j.apradiso.2012.11.014
786 Solaja, O., Omodehin, A., Badejo, B. 2017. Socio-ecologies of solid waste in Ijebu-Ode, Ogun
787 State, Nigeria. ReciklazaiOdrziviRazvoj, 10(1), 1–8.https://doi.org/10.5937/ror1701001s
788 Tahri, M., Benyaich, F., Bounakhla, M., Bilal, E., Gruffat, J.J., Moutte, J., Garcia, D., 2005.
789 Multivariate analysis of heavy metal contents in soils, sediments, and water in theregion of
790 Meknes (central Morocco). Environ. Monit. Assess. 102, 405–417. http://
791 dx.doi.org/10.1007/s10661-005-6572-7.
792 Taskin, H., Karavus, M., Ay, P., Topuzoglu, A., Hidiroglu, S., Karahan, G. 2009. Radionuclide
793 concentrations in soil and lifetime cancer risk due to gamma radioactivity in Kirklareli ,
794 Turkey. *Journal of Environmental Radioactivity*, *100*(1), 49–53.
795 http://doi.org/10.1016/j.jenvrad.2008.10.012
796 Tian, K., Huang, B., Xing, X., Hu, W., (2017). Geochemical baseline establishment and ecological
797 risk evaluation of heavy metals in greenhouse soils from Dongtai, China. Ecol. Indic. 72,
798 510–520.
799 UNSCEAR, 2000. Sources and Effects of Ionizing Radiation. United Nations scientific Committee
800 on the Effects of Atomic Radiation.Vol.1 New York.United Nations,
801 US EPA, 2001. Risk assessment guidance for superfund. In: Process for Conducting Probabilistic
802 Risk Assessment. vol. III - Part A US Environmental Protection Agency, Washington, DC
803 (EPA 540-R-02-002).
804 US EPA, 2002. Supplemental Guidance for Developing Soil Screening Levels for Superfund Sites.
805 Office of Solid Waste and Emergency Response, Washington, DC (OSWER 9355.4-24).
806 Wadey, P., Hu, Q., Minski, M.J., and Shaw, G. 1991. Soil-to-plant transfer of radionuclides-
807 lysimeter-based studies at Imperial College. Environ. Geochem. Health, 13: 139-140.

World Health Organization [WHO], 1993. Evaluation of Certain Food Additives and Contaminants. In: Forty-First Report of the Joint FAO/WHO Expert Committee on Food Additives. WHO, Geneva, Switzerland (WHO Technical Series, 837).

Zach, R., 1982. Limcal-A Comprehensive food Chain Model for Predicting Radiation Exposure to man in Long-term Nuclear Waste Management. Atomic Energy Canada Limited, Mississauga, ON., Canada.

Zhang, Z., Juying, L., Mamat, Z., QingFu, Y. , 2016.Sources identification and pollution evaluation of heavy metals in the surface sediments of Bortala River, Northwest China Ecotoxicol. Environ. Saf., 126 (2016), pp. 94-101

Zhou, Z., Yang, Z., Sun, Z. *et al.* 2020. Multidimensional pollution and potential ecological and health risk assessments of radionuclides and metals in the surface soils of a uranium mine in East China. *J Soils Sediments,* 20: 775–791 (2020). https://doi.org/10.1007/s11368-019-0242

820

821